Swing-arm Profilometry of Aspherics

David S. Anderson and James H. Burge
Steward Observatory Mirror Lab
University of Arizona
Tucson, Arizona 85721

Abstract

A profilometer is described that utilizes the swing-arm geometry to provide surface profile measurements of large, highly aspheric surfaces. The profilometer measurement is shown to be robust against stiffness and alignment induced errors in the probe motion.

Keywords: profilometry, aspheric testing, surface profile

Introduction

The rapid and economical fabrication of highly aspheric surfaces having aspheric departures of more than 100μ generally demands that the aspheric departure be ground into the surface and not polished in as can be done with surfaces having lesser departure. Measurements of the ground asphere as the surface is being worked can be a difficult task particularly when the surfaces are large, convex aspheres commonly found on large telescope secondary mirrors such as those being fabricated at the Mirror Lab. The basic fabrication strategy for these secondary mirrors will be to generate and grind the surface to a sphere, then lap in the aspheric correction with loose abrasives using the stressed-lap. When the asphere is about 90% corrected polishing will begin and the correction completed. The surface will be tested interferometrically with a holographic test plate for the final figuring.

To monitor the aspherization a swing-arm profilometer mounted directly on the polishing machine will be used until the surface is within 1 micron p-v of the finished asphere. The ability to measure *in situ* is a tremendous advantage of this type of profilometer. In addition, the profilometer will measure the surface under complete computer control allowing for both rapid and repeated testing.

In a previous paper[1] the swing-arm profilometer was first described and an example of its use was shown. In this paper we will elaborate on the design features of this somewhat odd geometry that make it so useful in fabricating aspherics and estimate its accuracy. We will also point out some of the limitations of this form of profilometer.

Swing-arm Geometry

Figure 1 depicts the basic geometery of the swing-arm profilometer. An indicator (i) mounted at the end of an arm (a) that itself pivots on a rotary bearing (b) sweeps out a circle in space like a compass. If the axis of rotation of the rotary bearing is tilted with respect to the symmetric axis of a spherical surface such that the two axes intersect at the center of curvature of the sphere (cc), the circle that the indicator traces will lie on the surface of the sphere when the indicator passes through the vertex (v) of the sphere. As the indicator sweeps across the spherical surface it would show no run-out given a perfectly stiff arm and perfect bearing. The angle of the required tilt is given by

$$\sin\theta = l/R$$

where l is the length of the arm (the perpendicular distance from the arm's axis of rotation to the tip of the indicator), and R is the radius of curvature of the sphere.

The indicator is initially aligned at the vertex of the mirror to be normal to the surface. For a spherical surface the indicator will always be directed normal to the surface since it is being pivoted about

the center of curvature. When measuring an aspherical surface the only distance the indicator measures is the amount of asphericity in the direction of the probe along with any alignment or flexure errors. (See Reference 1 for an analysis of the measurement for a perfect profiler). This requires that the probe travel only be as long as the amount of asphericity in the mirror. This allows the use of relatively inexpensive LVDT probes.

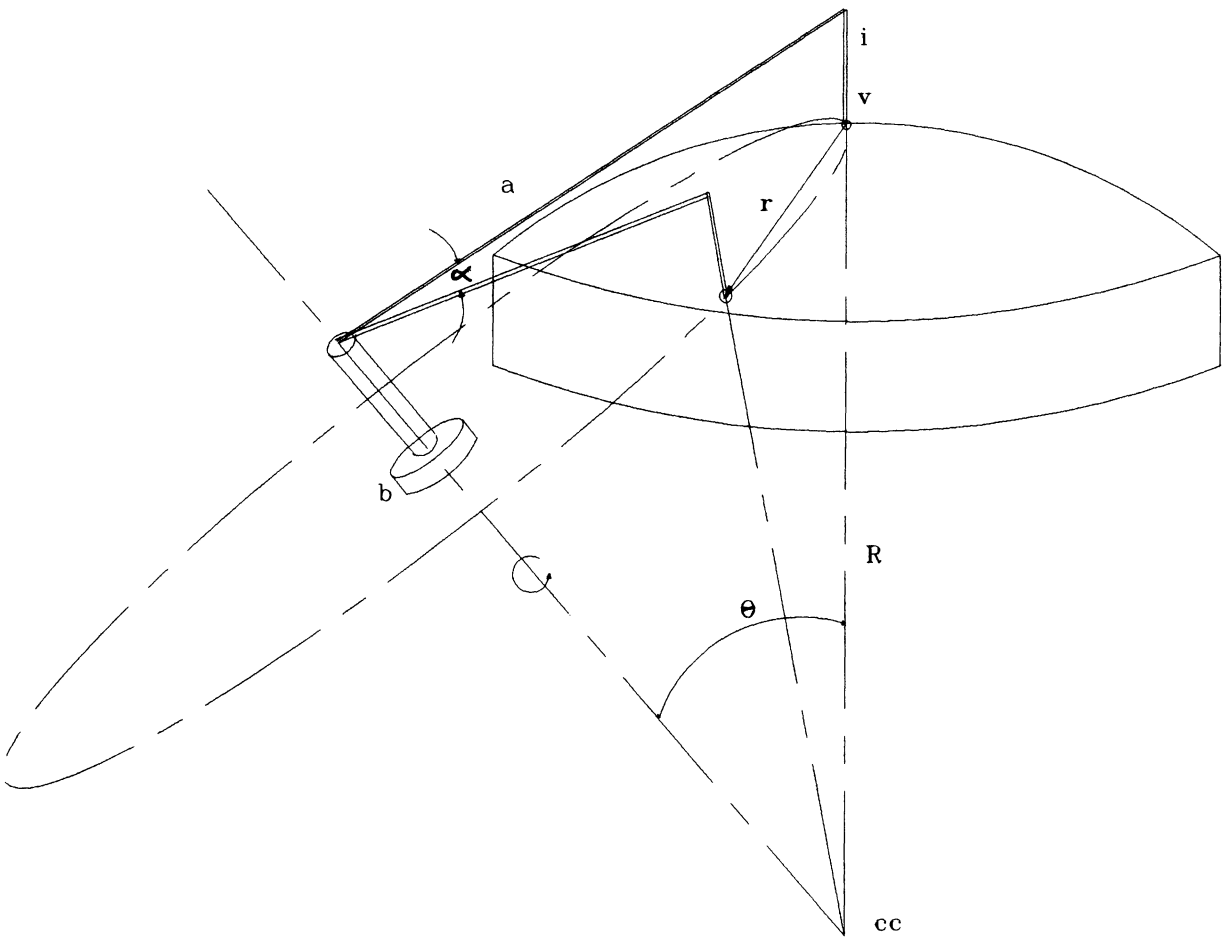

Figure 1. The basic geometry of the swing-arm profilometer. The indicator (i) is mounted on arm (a) pivoting about the bearing (b). The rotation axis of the swing-arm is aligned to intersect the center of curvature of the surface.

The rotary motion of the swing-arm is the only mechanical motion of the profilometer during a measurement (along with the motion of the indicator). Modern rotary bearings, especially air bearings, are highly stiff with excellent smoothness that allow highly accurate measurements to be made. The center of gravity of the arm assembly is adjusted with counterweights to lie on the bearing's axis resulting in a decoupling of the measurement with the stiffness of the bearing.

Unlike linear profilometers, the path scanned by the swing-arm profilometer is not a straight line across a diameter but is an arc. As an example, in Figure 2 is shown the path taken by a swing-arm

profilometer having an arm length of 1.5 m over the surface of the f/4 secondary mirror for the Large Binocular Telescope (LBT). The mirror is 1236 mm in diameter and has an f/1.5 surface with nearly 350μ departure from the best-fitting sphere. Although the path is curved the radial position varies nearly linearly with the scan angle as shown in Figure 3. The departure from linear of this α *vs* r plot is only 0.4%.

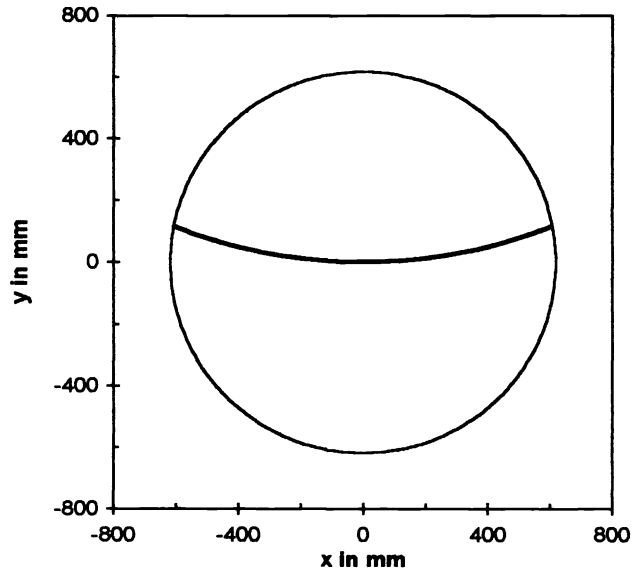

Figure 2. The arc scanned on the LBT f/4 secondary by a profilometer with a 1.5m length arm.

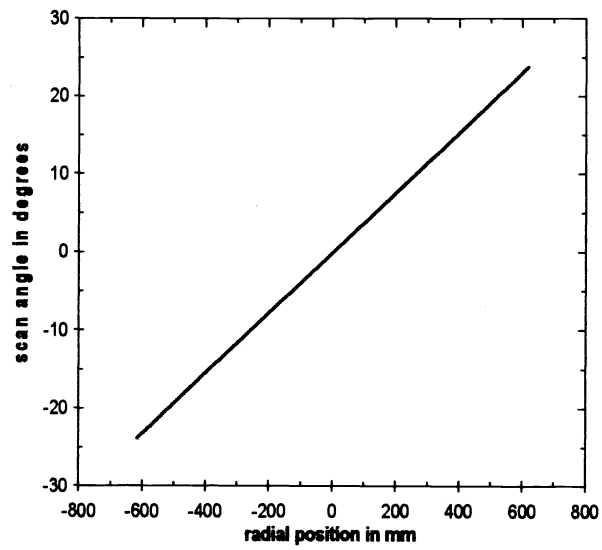

Figure 3. The radial position varies linearly with the scan angle.

General structure

Figure 4 depicts a schematic design of a practical swing-arm profilometer based on the geometry of Figure 1. The main structural elements are the indicator assembly, the main arm, the swing-arm rotary bearing, and the swing-arm alignment assembly. We will briefly discuss each.

1. The indicator assembly

The indicator assembly consists of a sub-arm that pivots at the junction of the main arm to bring the indicator roughly normal to the surface. The indicator is mounted on a 5-axis stage so that the indicator can be accurately positioned at the center of the mirror, brought normal to the surface, and the indicator brought within its range. As mentioned, the indicator travel need only be that of the amount of asphericity. Because of that the cosine error resulting from a non-normal set-up is extremely small. Also, since the probe is always normal to the surface (or very nearly so) there is very little error due to the contact point moving during a scan. As discussed below, the mass of the assembly should be kept as low as possible and the arm and stages should be as stiff as possible to minimize the deflection during a measurement.

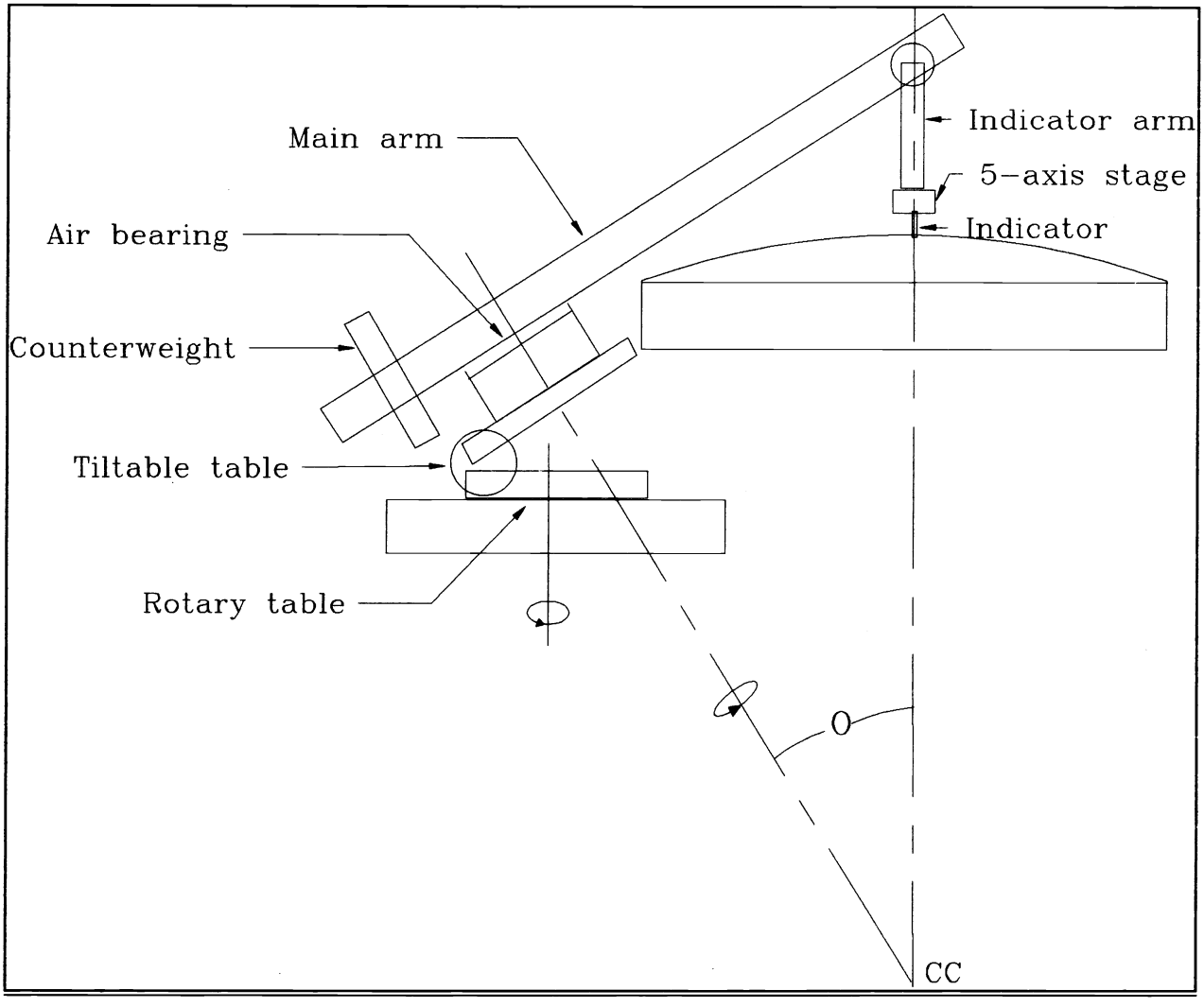

Figure 4. A schematic diagram of the swing-arm profilometer.

2. The main arm.

The principal requirement of the main arm is that it be stiff enough to resist a large change in deflection as it is scanned across the surface. It can be shown that the measurement is quite tolerant of some flexure in the arm. The effects of the arm flexing and of the indicator's arm flexing under the force of gravity were studied using a first order model. We calculate that the system does not require high rigidity to achieve excellent performance because the flexure is generally in the form of power, which, as in interferometry of curved surfaces, is coupled into an alignment error, here being the tilt of the bearing axis. We used a simple model of the system that takes into account all the important masses and flexures.

The model breaks the system into two lumped masses. One is near the end of the arm and the other is at the probe. We then model two three-dimensional stiffness elements. One corresponds to the arm and the other corresponds to the attachment of the probe to the arm. If the effective masses of these two elements are determined and the stiffness is measured, then the system flexure can be calculated in a straightforward manner. The geometry and the coordinates used are shown below in Fig. 5. The unprimed coordinate system is fixed, while the xyz' is tilted θ to vertical and the xyz" system which is fixed to the probe and swings the angle α with the air bearing. This system is also tipped back so that the probe points along the z" axis.

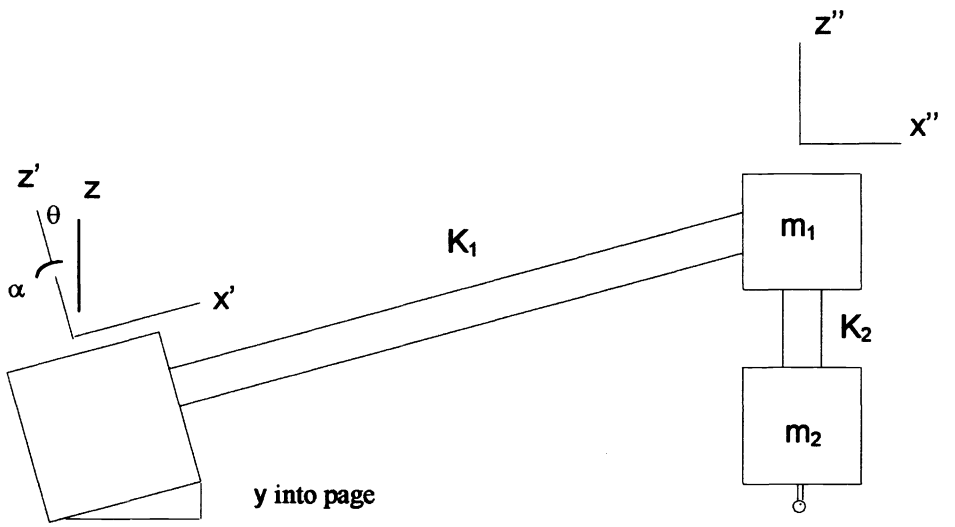

Figure 5. Diagram showing model for structural analysis.

The four modes were treated: the motion of masses 1 and 2 together in y and in z, and the differential y and z motion. A matrix formalism was adopted for easy manipulation. The stiffness matrices K_1 and K_2 are defined as the ratio of force to probe displacement $\delta y''$ and $\delta z''$ when forces are applied to m_1 and m_2 in the y" and z" directions

$$K_{1y} = \frac{F_{1y}}{\delta y''}, \quad K_{1z} = \frac{F_{1z}}{\delta z''}$$

$$K_{2y} = \frac{F_{2y}}{\delta y''}, \quad K_{2z} = \frac{F_{2z}}{\delta z''}.$$

These can be measured directly by pulling with a known force and measuring displacement at the probe tip with an indicator. We do not treat flexure in the x direction because it does not affect the measurement.

The algebra reduces to two expressions relating the motion of the probe tip in y and z to the angles.

$$\delta y'' = \left(\frac{m_1 g + m_2 g}{K_{1y}} + \frac{m_2 g}{K_{2y}} \right) (\sin\theta \sin\alpha)$$

$$\delta z'' = -\left(\frac{m_1 g + m_2 g}{K_{1z}} + \frac{m_2 g}{K_{2z}} \right) (\sin^2\theta \cos\alpha + \cos^2\theta)$$

Since the resonant frequency in rad/sec is given by the square root ratio of the stiffness to the mass, the deflections can be expressed purely as functions of these frequencies and the angles,

$$\delta y = \left(\frac{1}{4\pi^2 f_{1y}^2} + \frac{1}{4\pi^2 f_{2y}^2} \right) g \sin\theta \sin\alpha$$

$$\delta z = -\left(\frac{1}{4\pi^2 f_{1z}^2} + \frac{1}{4\pi^2 f_{2z}^2} \right) g (\sin^2\theta \cos\alpha + \cos^2\theta)$$

where f_{1y} and f_{1z} are the natural frequencies in Hz of the arm in the *y"* and *z"* directions
f_{2y} and f_{2z} are the natural frequencies of the end of the arm in the *y"* and *z"* directions

These relationships were simulated to determine the exact nature of the errors that come from system flexure. The simulation shows that this effect can be quite severe, but that the method of determining the arm length using the outer edge of the optic as a reference eliminates the error. The two equations above show the radial position varying with the sine of the scan angle, which is nearly linear with the radial position itself. This motion causes spherical aberration in the measurement corresponding to conic constant change ΔK

$$\Delta K = 4K \frac{\Delta r}{r}.$$

The other term involving *z* goes as the cosine of the angle, which looks like nearly pure quadratic power in the measurement. Assuming a 10 Hz resonance in both z and y, we predict 35 μm quadratic bending and 3.4 μm spherical aberration. However, we use the mirror diameter and the scan angle to determine the arm length. Unlike linear scanning profilometers the radial position of a data point is not measured directly but is calculated from a knowledge of the angle from the center of the surface and the length of the arm. The test requires the distance from the probe to the rotation axis, which we call the arm length, be known to a fraction of a millimeter. This distance can be determined by scanning the probe across two points separated by a known distance *D*. The arm length *l* is calculated to be

$$l = \frac{D}{2\sin\left(\frac{\alpha}{2}\right)}$$

where α is the angle swept between the two points, as measured by the encoder on the bearing. The edges of the mirror are used as the two points since the diameter of the mirror can be accurately measured and the edges can be easily located. This calibration must be done after any adjustment of the probe since that changes its distance from the rotation axis.

This bending will cause an error in the calculation of the arm length that offsets the scan error. The reason for this is that by using the known edge locations, the error in the radial position Δr/r is corrected. This is seen in Fig. 6 which shows the error in radial position from this flexure for the two cases described: assuming the true arm length is known and used and assuming the arm length is determined by referencing the edge of the part.

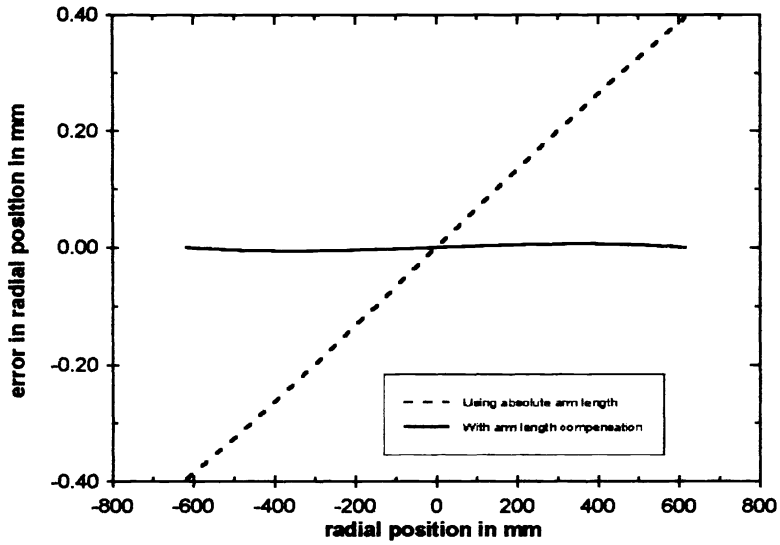

Figure 6. Error in radial position due to flexure of system with 10 Hz resonance for two cases: scanning with a known arm length, and using the outer diameter to determine the arm length.

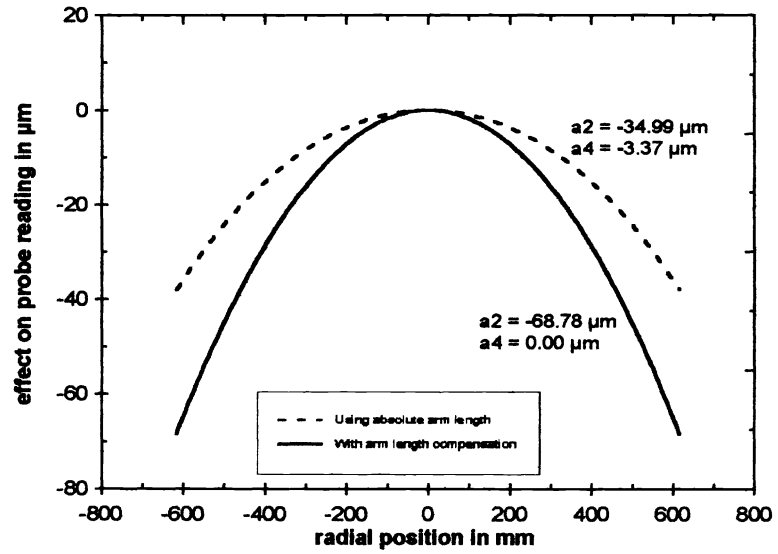

Figure 7. Effect of system flexure (10 Hz in z and y diections) on suface measurement. The solid curve which assumes the arm length is determined by scanning to the two edges of the part shows negligible spherical aberration.

3. The rotary bearing.

The swing-arm rotary bearing is the crucial moving element in the profilometer. The high stiffness and precision of modern air bearing spindles provide an excellent bearing for this task. Radial runouts of less than a micron are typical and produce negligable error in the measurement .

Axial runout is of much greater concern, however, since this type of error couples directly into the measurement and is magnified by the length of the arm. Smoothly varying axial runout such as a sinusoidal variation can be largely eliminated by fitting the data to tilt and focus and removing them from

the data. Higher frequency structure in the axial runout will couple in directly to the measurement. Air bearings having axial runouts on the order of .1 microradians produce less than .15μ error in the measurement over a 1.5m arm length. If these errors are repeatable they can be calibrated out by measuring a known standard such as the spherical surface prior to aspherizing. If the errors are random, averaging many measurements will reduce the error.

The rotary bearing must be precisely driven and encoded to provide positional information during a measurement and also to determine the length of the arm. The accuracy required for the f/4 LBT secondary is about 25 microradians corresponding to about 38 microns at the end of a 1.5 m arm. Tests are currently underway on an encoder/drive system from Dover that are expected to easily meet this specification with a fully computer controlled interface.

4. The alignment axes.

There are two alignment axes that allow the swing-arm bearing axis to pass through the center of curvature of the surface. The first is a tilt axis to tilt the bearing axis through the angle θ in Figure 5. If this angle were well known the profilometer could, in principal, measure the radius of curvature of the surface. The knowledge of this angle alone, however, will not result in the right radius since the arm deflections and indicator misalignments also couple into the power term of a polynomial fit to the data. The exact radius of curvature of the surface must be determined by other means. We intend to use small aperture test plates to monitor the radius within acceptable limits.

To align the profilometer the angle is set to the calculated value for the particular desired radius and a scan is made over the surface. The power term of a polynomial fit to the data is used to adjust the angle until the power term is sufficiently small, on the order of a few microns. Absolute knowledge of the angle is not required only that it be adjustable to about an arcminute or so.

The second alignment axis is provided by a second rotary axis having its axis parallel to the optical axis of the surface. This adjustment allows the tilted axis to intersect the optical axis of the mirror at its center of curvature. This can be provided by a suitably sturdy rotary table. This, again, does not need to be a particularly precise bearing, only that it be adjustable to a few arc minutes. During alignment, when a scan is made, the data can be fit to a linear term that provides information on the required adjustment to be made with this rotation.

Sensitivity to errors.

The sensitivity to alignment errors was determined by computer simulation. A computer model was constructed that simulates the rotation of the probe about a fixed axis. The probe reading as a function of scan angle is calculated by projecting a line in the direction the probe points to intersect the optical surface. This general model allows the complete system to be simulated and analyzed. The computer model was used to determine the effects of misalignment, measurement errors, and system flexure. The model was verified to give the same result as the above equations for the ideal case.

Simulation were performed for the measurement of the f/4 LBT secondary previously described. The simulated indicator reading as a function of radial position is shown in Fig. 9. Two cases were simulated, one with the tilt angle set to 23.99° from vertical so the paraxial power is removed from the scan. The other curve assumes a tilt angle of 23.35° which minimizes the probe travel.

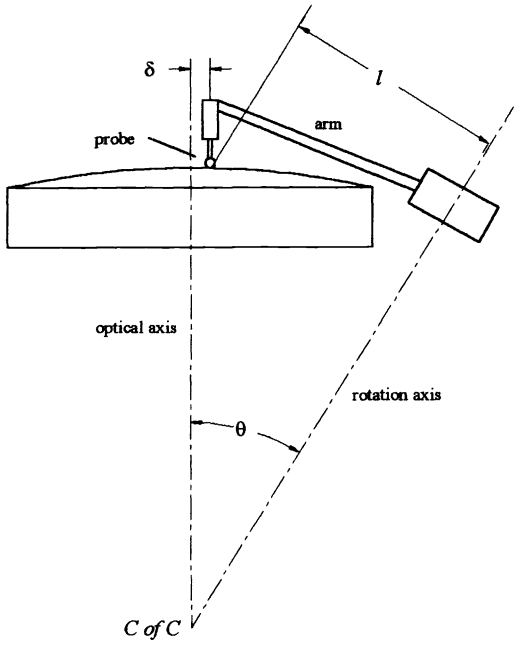

Figure 8. Side view of test configuration for measuring a convex optic showing the misalignment δ of the probe.

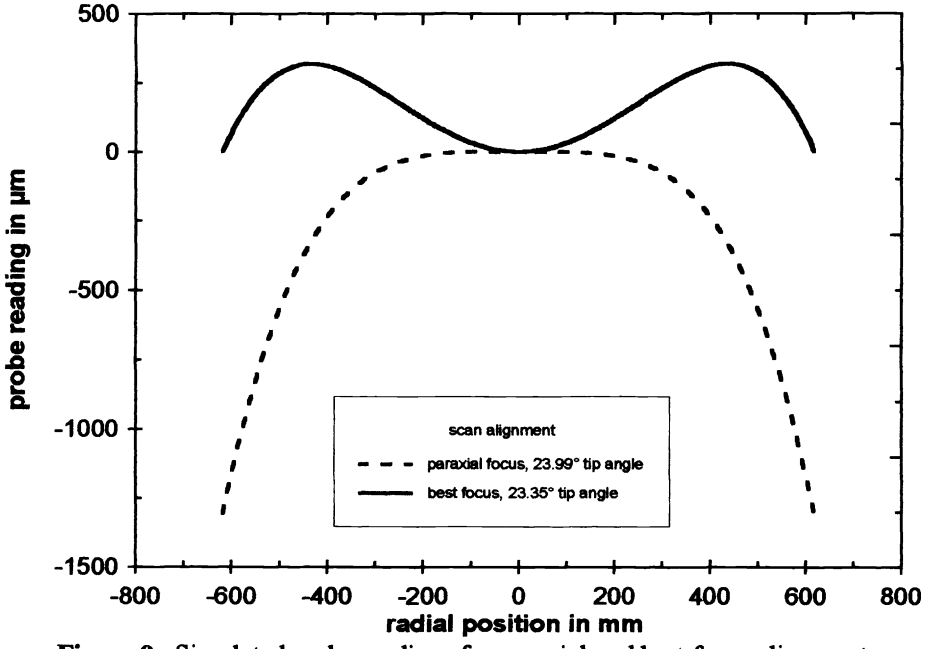

Figure 9. Simulated probe readings for paraxial and best-focus alignment

The effect of a 100 µm error in defining the mirror vertex in the cross-scan direction is shown in Fig. 10. This offset is labeled δ in the drawing shown in Fig. 8. This curve shows mostly power, which is removed

by the tilt alignment. A polynomial fit to the curve shows 0.13 μm of fourth-order spherical aberration, which corresponds to a conic constant shift of 96 ppm.

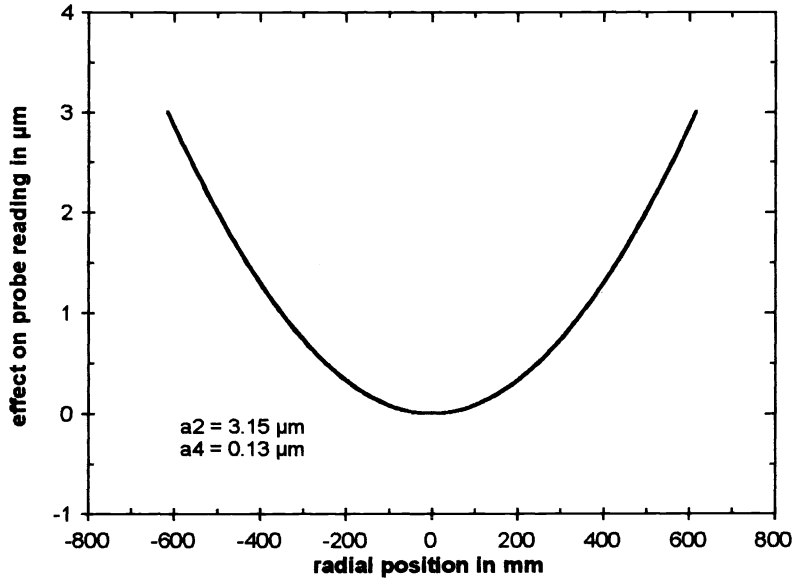

Figure 10. Simulated error in measurement when the scan is offset 100 μm from the mirror vertex.

The effect of a 200 μm error in the arm length, which could come from 80 μm errors in locating the two reference points, is shown in Fig. 11. This curve also shows mostly power. A polynomial fit to the curve shows 0.61 μm of fourth-order spherical aberration, which corresponds to a conic constant shift of 0.00045. The error in the arm length Δl is calculated from the error in determining the distance between the two reference points ΔD as

$$\Delta l = l\frac{\Delta D}{D}$$

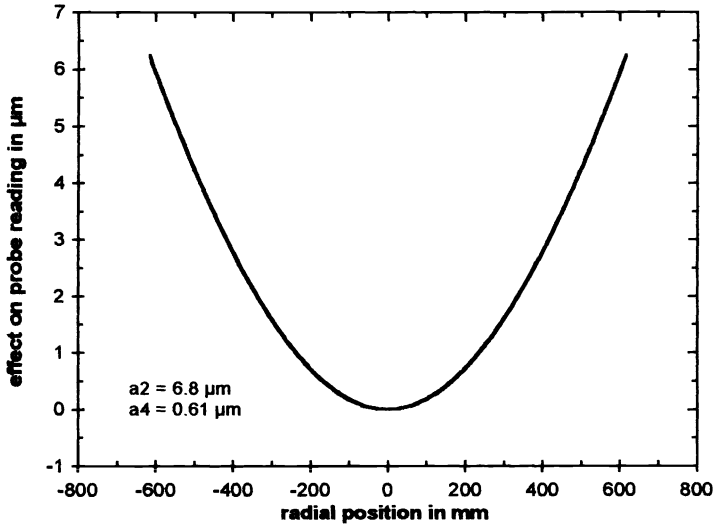

Figure 11. Simulated error in measurement when the arm length determination is in error by 200 μm.

Changing the tilt stage causes nearly pure power, or quadratic variation in the measurement. A plot of the simulated change in surface measurement with a tilt change of 1 mrad is shown in Fig 12. This angle corresponds to a change of the effective radius of curvature of 8.5 mm.

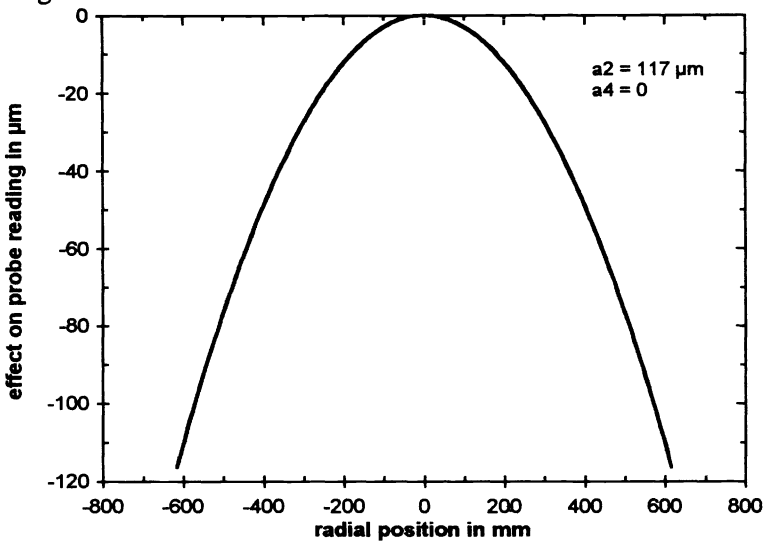

Figure 12. Simulated error in measurement when the table is tilted 1 mrad.

Conclusions

We have reviewed the basic structure of the swing-arm profilometer and have discussed why the profilometer can measure aspherics as accurately as it has been demonstrated it can do. Most of the error induced by the various mialignments and flexures couple into tilt and power and not into spherical aberration, the quantity we wish to measure. The price for this robustness is the loss of information about the radius of curvature of the surface. It must now be determined by other means.

The advantages of this type of profilometer include:

1. Capable of performing *in-situ* measurements on the polishing machine.

2. Relatively economical to construct. The measurement probe can be a short travel LVDT and the only precision moving part is an air bearing spindle.

3. The stiffness requirements are modest since small deflections cause power error in the measurement.

4. Accuracy is quite high, < 1µ P-V over large, severe aspheric surfaces. Chiefly limited by the determination of the arm length.

The disadvantages of this type of profilometer:

1. The arm length must be recalibrated if any alignment adjustments are made.

2. The radius of curvature is indeterminent.

References

1. Anderson, D.S., Parks, R.E., Shao,T., "A versatile profilometer for the measurement of aspherics," OF&T Workshop Technical Digest, Monterrey, CA 1990.